©*Proc. Indian natn. Sci. Acad.*, **52**, A, No. 1, 1986, pp. 25–47
Printed in India.

ADVANCED PHYSICAL METHODS FOR THE CHARACTERISATION OF POWDERS*

A K CHEETHAM

University of Oxford, Chemical Crystallography Laboratory, 9 Parks Road, Oxford, U.K.

A wide range of physical methods is now available for the study of powder materials. Recent advances in some of these methods, including analytical electron microscopy, magic angle spinning NMR, and powder diffraction with X-ray and neutrons, are described, and the scope and limitations of the techniques are discussed.

Key Words : Physical Methods; Electron Microscope; Magic Angle Spinning NMR; Powder Diffraction with X-rays and Neutrons

1. INTRODUCTION

THE need for new materials for a wide range of applications, including catalysis, energy storage, and solar conversion, is widely recognised,[1] but it is probably true that our ability to prepare such materials now exceeds our ability to characterise them. Most new materials that reach the stage of commercial application will be used in the form of powders, but in many cases the initial characterisation has been carried out by using single crystals. Typically, this vital step involves a definitive structure determination by X-ray diffraction. For materials that can only be made in powder form, however, the route to complete characterisation is more precarious. Traditionally, X-ray powder diffraction will be used to identify a new phase, but if the pattern is complex, it may be difficult to index it and determine the crystal system and lattice parameters. Under these circumstances, very careful work is required even to confirm that the material is a single phase, and it is not unusual for the composition, determined by bulk chemical analysis, to be incorrectly assigned. Even if the X-ray pattern can be indexed, problems can still arise. To take a recent example, the composition of the sodium conductor NASICON, which was first reported in 1976,[2] has been the subject of a great deal of discussion.[3] In instances where the powder pattern cannot be indexed, the likelihood of obtaining a full structure is remote, and in many cases this will preclude further development of the material. For example, the potential of a new zeolitic material for shape-selective catalysis is determined almost entirely by its structure, and it is clearly a great disadvantage if this is unknown. In order to take full advantage of the many exciting developments in synthetic chemistry, it is therefore essential that proper attention should be paid to the improvement of physical methods.

*Presented at the INSA Golden Jubilee Symposium on 'Solid State Chemistry' held at INSA, New Delhi during 4–6 December 1985.

The purpose of this paper is to describe some of the advanced methods that are now available for the characterisation of powders. In the last decade, substantial progress has taken place in many areas. Analytical electron microscopy offers the possibility of determining the compositions of the constituent phases in even the most complex mixture.[4] High resolution powder diffraction methods, especially using neutrons, are now able to solve structures *ab initio*[5]; and magic-angle spinning techniques have brought the power of nuclear magnetic resonance to the solid state.[6] These, and other methods that can be applied to the study of powders, are discussed in the following sections.

2. Analytical Electron Microscopy

2.1 *Introduction*

The first step in the characterisation of a powder sample is the determination of the composition of the phase or phases that are present, and it is here that the analytical electron microscope can play a unique role. A modern transmission electron microscope is a very versatile instrument, offering a wide range of modes in addition to diffraction and imaging. These can best be understood by examining some of the many ways in which the electron beam can interact with the specimen (Fig. 1). The modes that are of particular relevance to the study of powders are reviewed in the following sections.

Transmission Electron Microscopy (TEM, diffraction): Electrons are normally generated by thermionic emission from a cathode filament, often tungsten, and monochromated by acceleration through a potential, E. For an accelerating voltage

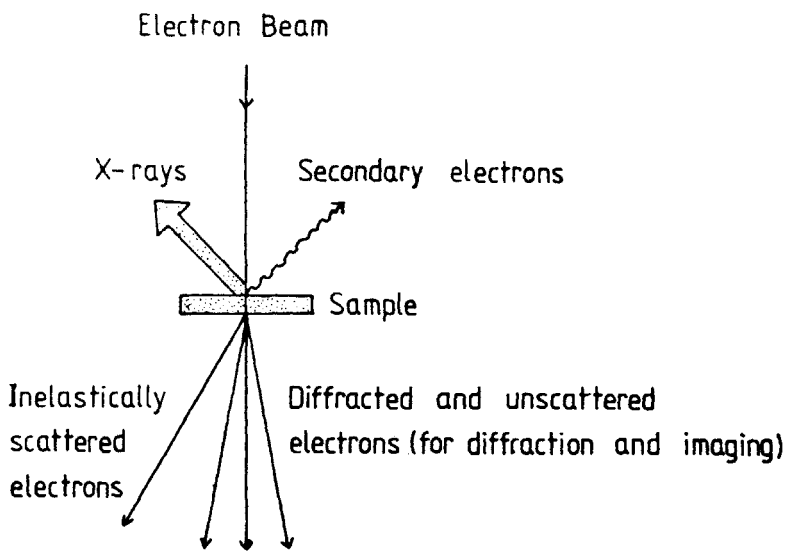

FIG 1 Some of the important interactions between an electron beam and a specimen.

of 100keV, the wavelength is 0.037Å. Electrons may be elastically scattered by the atomic potentials of the atoms in the specimen, leading to the formation of a diffraction pattern for a selected area of crystalline material. This can provide useful information concerning the lattice parameters and crystal system of the material. The diffraction pattern may, in turn, be transformed by a magnetic lens into an image of the specimen, a step that requires human intervention and a great deal of computing with X-rays. The use of high resolution electron microscopy to obtain images with atomic resolution will be discussed in a later section.

Scanning Electron Microscopy (SEM, STEM) : The low energy electrons (less than 50eV) that are emitted from the surface of the specimen during electron irradiation form the basis for a different type of imaging. The beam may be concentrated to a small probe (say 20Å diameter) that can be deflected across the specimen in a faster fashion using scanning coils. The secondary electrons can be detected above the specimen, and an image showing the intensity of secondary electrons emitted from different parts of the specimen surface can be displayed on a CRT. This SEM mode is particularly useful for examining the morphology of a crystal surface.

A related technique involves the collection of electrons that are transmitted through the specimen during scanning. These can be used to produce a scanning transmission (STEM) image, with the advantage, compared with TEM, that radiation damage is reduced because the beam is not stationary.

X-ray Emission Spectroscopy : One of the most important interactions between the electron beam and the specimen is the stimulation of characteristic X-ray emissions from the elements present. These can be detected and sorted into different energies by using a crystal monochromator or an energy dispersive detector. X-ray detection has been used for many years on scanning microscopes (the microprobe), but only recently has it found widespread use on transmission instruments. The resulting spectra (*see* Fig. 2) are extremely valuable for chemical analysis of powders.

The intensities of the spectral lines can be related quantitatively to the composition of the sample. For thick specimens (the usual microprobe situation) :

$$C(x) = k.Z.A.F.I(x), \qquad \ldots(1)$$

where $C(x)$ is the concentration of element x, k is a constant, Z is an atomic number correction, A is an absorption correction, F is a fluorescence correction, and $I(x)$ is the intensity of a characteristic X-ray emission of x.

For thin specimens (the typical TEM situation) :

$$\frac{C(x)}{C(y)} = k_{xy} \frac{I(x)}{I(y)} \qquad \ldots(2)$$

The method requires a standard compound in order to determine the value of k_{xy}, but once this has been established for a particular pair of elements (on a given

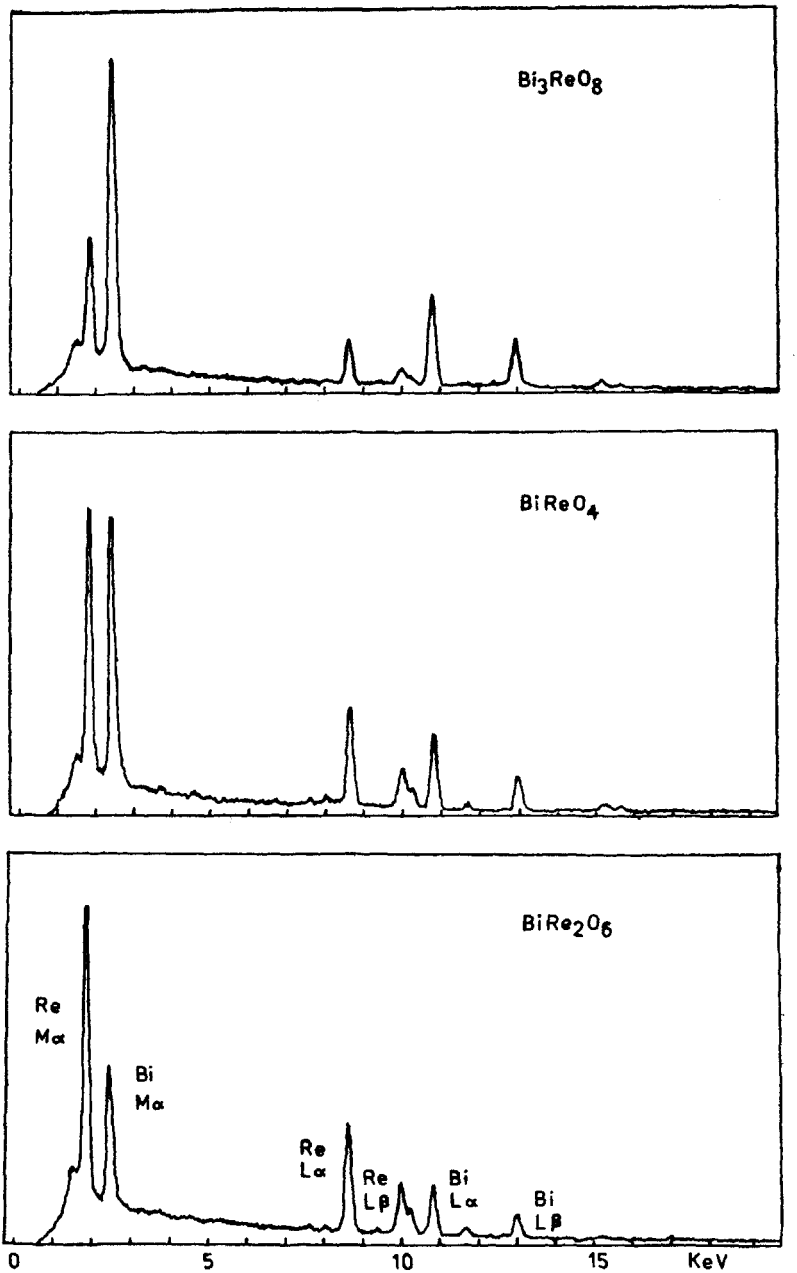

FIG 2 X-ray emission spectra obtained from thin crystals of Bi_3ReO_8, $BiReO_4$, and $BiRe_2O_6$ at 100 KeV on a Jeol 100CX TEMSCAN instrument.[8] The Cu lines arise from the supporting grid.

instrument), the same value can normally be used for any other compound containing those elements.

Electron Energy Loss Spectroscopy (*EELS*): Energy loss spectroscopy looks at inelastically scattered electrons that have lost energy in the sample due to a range of processes, including plasmon excitations and the ionisation of core electrons; the latter is the preliminary step in X-ray emission. A typical spectrum is shown in Fig. 3. The sharp peaks on the L-edge of vanadium stem from electric dipole transitions between the $2p$ and $3d$ levels. It has been shown that the ratio of the intensities of these peaks is a function of the number of d electrons, and therefore the oxidation state.[7] The position of the edge is also affected by the oxidation state.

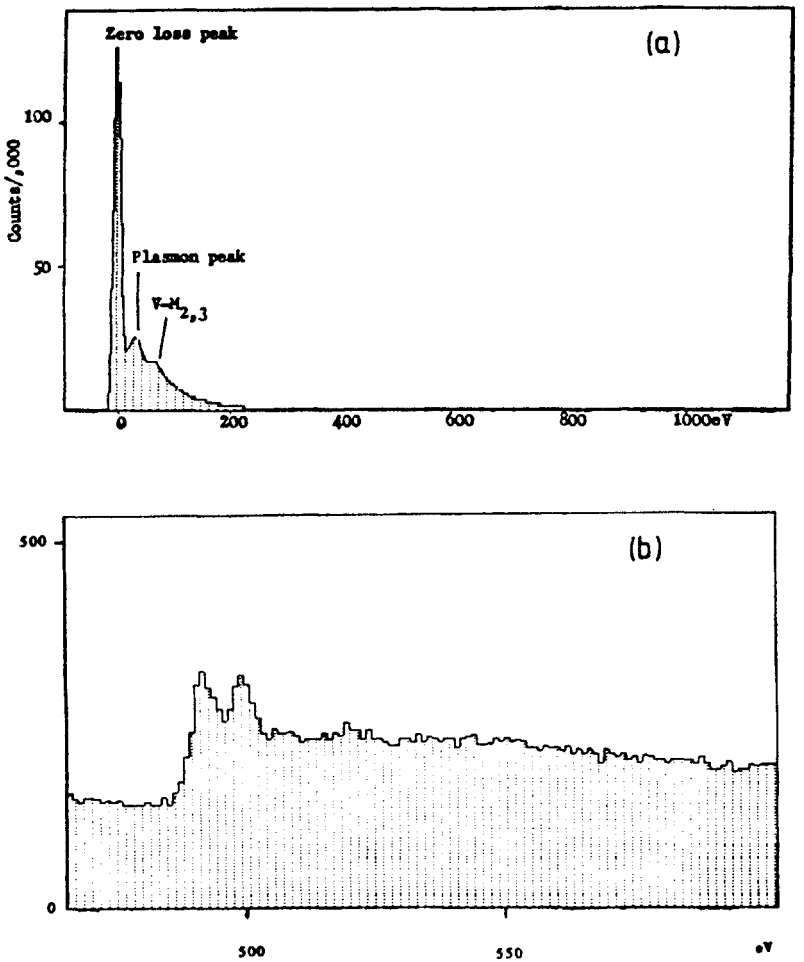

FIG 3 Electron energy loss spectra of a vanadium oxide, obtained at 200KeV on a Jeol 2000FX TEMSCAN instrument—

(a) Full spectrum, 0–1100eV range.

(b) Detail at the vanadium L-edge, showing the $L_{2,3}$ fine structure (Cheetham and Starr, *unpublished*).

The EELS method is the most sensitive in the 0–1000eV range, a range that includes the K-edges of the elements H-F, and is therefore useful for analysing light elements that are not always detected in X-ray emission spectroscopy. Elemental maps may also be obtained in the form of energy filtered images.

2.2 *Applications*

The applications of analytical microscopy in solid state chemistry have been reviewed by Cheetham and Skarnulis.[4] The major advantage is that chemical compositions can be determined with very high spatial resolution by utilising the magnifying power of the instrument. This permits the compositions of the phases that make up a complex mixture to be examined individually, thus facilitating phase identification. An important area of use is in synthesis, where the traditional approach of powder X-ray diffraction, though invaluable in many instances, can be rather uninformative if the patterns of the product phases are entirely new. The electron microscope enables us to probe the compositions of the phases, directly. For example, in a study of the system Bi–Re–O, Rae-Smith and Cheetham[8] were able to identify three new compounds in the product of a single reaction between Bi_2O_3 and ReO_3 : Bi_3ReO_8, $BiRe_2O_6$, and $BiReO_4$. The X-ray emission spectra are shown in Fig. 2. Note that in this case, the Bi : Re atomic ratio of each phase can be deduced by simple inspection of the Bi(M): Re(M) intensity ratio. The methodology is to identify the compositions of the compounds present in the mixture and then to prepare each one in a pure form for further characterisation. Another area of use is in the elucidation of phase diagrams, where the tie-lines can be constructed from the compositions of the phases that are in equilibrium. A simple illustration is the use of AEM to establish the mutual solubilities of FeS_2 and MnS_2 in the solid state.[9]

A close inspection of Fig. 2 reveals that the X-ray emission spectra do not yield the compositions of the new oxides without ambiguity, since the oxygen K line cannot be observed due to absorption by the detector window. It is typically the case that the emissions from elements lighter than sodium (i.e. $<$ 1Kev) will be unobserved. In the Bi–Re oxides, therefore, only the Bi : Re ratios could be determined, and other information was required in order to complete the analysis. $BiReO_4$ and $Bi_3Re_3O_{11}$, for example, give indistinguishable X-ray spectra.[10] Recently, a new type of thin window X-ray detector, which extends the elemental range down to carbon, has become available, and the early indications are that quantitative oxygen analysis should be possible with such devices.[11,12] Fig. 4 shows a typical spectrum obtained with a thin window detector, and Fig. 5 confirms that metal : oxygen ratios can be obtained by using the thin crystal approximation.

An alternative approach to light element analysis involves electron energy loss spectroscopy. Loss peaks from the first row elements, Li–Ne, fall in the most sensitive part of the EELS spectrum, between 0 and 1000eV, and quantitative metal : oxygen ratios have been obtained by measuring the areas under the appropriate edges.[13] More directly, it may be feasible to assign the oxidation state of, say, a transition

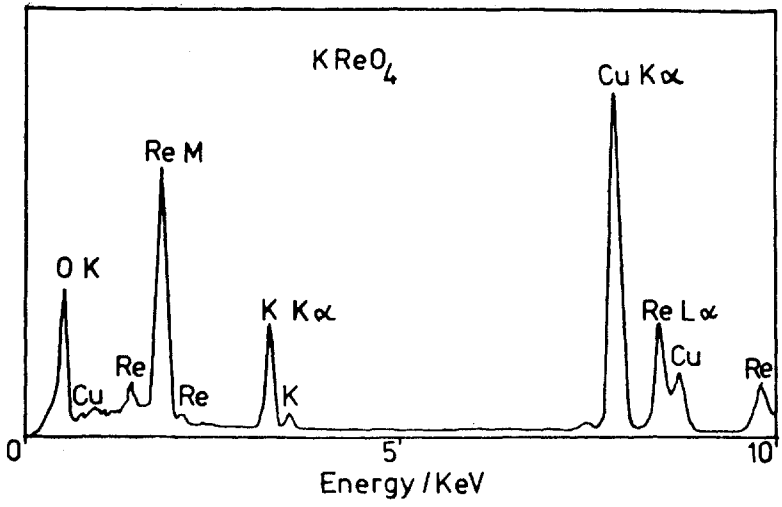

FIG 4 X-ray emission spectrum of $KReO_4$, obtained at 200 KeV on a Jeol 2000EX TEMSCAN instrument equipped with a Tracor thin-window detector.[12]

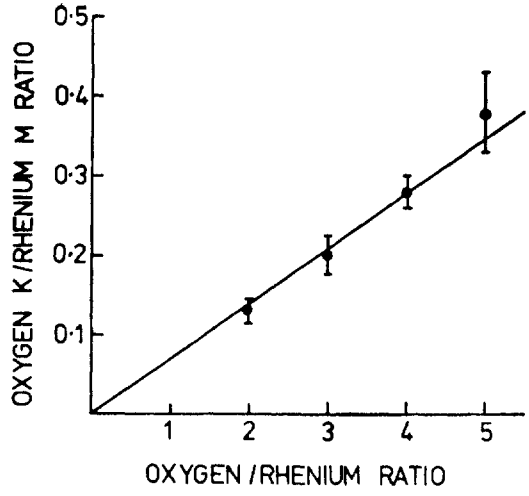

FIG 5 Oxygen K : Rhenium M intensity ratios, plotted versus oxygen : rhenium atomic ratios for a series of oxides : ReO_2, ReO_3, $KReO_4$ and Ba_2ReO_5.[12] The linearity of the results confirms that quantitative oxygen analysis can be obtained with thin crystals, according to equation (2).

metal by a careful study of its EELS peak. This has been attempted in two ways. First, the edge itself may exhibit a shift that depends upon oxidation state. For example, Rao *et al.* have shown that the *L*-edge of manganese, which corresponds to the ionisation of a 2s electron, varies smoothly in a series of binary and ternary oxides.[14] Second, the sensitivity of the L_3/L_2 intensity ratio to the number of *d*-electrons, which was described above, can, in principle, be used to determine oxidation states.

The power and versatility of AEM has already been demonstrated, but a great deal of potential still remains to be tapped. The EELS technique is only just beginning to make its mark on chemistry, and future developments in instrumentation and data processing are likely to enhance its capabilities in several ways. Particular attention will focus on the information content of the near-edge fine structure and the extended energy loss fine structure (EXELFS), which corresponds to the familiar EXAFS found in X-ray absorption spectra. Progress can also be expected in electron microscope design, leading to the availability of instruments on which both high resolution imaging and microanalysis can be performed simultaneously. At present, it is usually necessary to perform these functions on different instruments.

3. Magic Angle Spinning NMR

3.1 *Introduction*

Once the composition of a new material has been established, a wide range of physical methods is available for further characterisation. Diffraction methods, of course, play a vital role, but spectroscopic and reasonance techniques, including infrared, Raman, and UV-visible spectroscopies, and NMR, ESR, and Mössbauer measurements, can also provide valuable information. All of these methods are well established, but only recently has it become routinely possible to obtain high resolution NMR spectra from powders, by using the technique of magic angle spinning which was first proposed by Andrew and co-workers.[15]

NMR spectra of solids, in contrast to those of liquids, typically show broad absorptions in which the characteristic features of a solution spectrum—the chemical shift and spin-spin coupling information—are obscured. The purpose of the high resolution experiment is to remove these broadening effects whilst retaining the chemical information contained in the spectrum. Line broadening can arise from a range of anisotropic interactions.[16] Dipole-dipole interactions, between nuclei of the same element or between different spin types, are a common source of broadening, especially in hydrogen-containing materials. The effect is distance dependent ($1/r^3$) and can therefore be drastically reduced by dilution; for example, homonuclear dipolar broadening is not a problem with ^{13}C spectra. Heteronuclear interactions involving hydrogen are normally removed by broad band decoupling. A second important effect arises from the unsymmetrical nature of the chemical shift : the chemical shift anisotropy. In a single crystal experiment, the chemical shift of the resonance depends upon the orientation of the crystal, and thus the magnetic

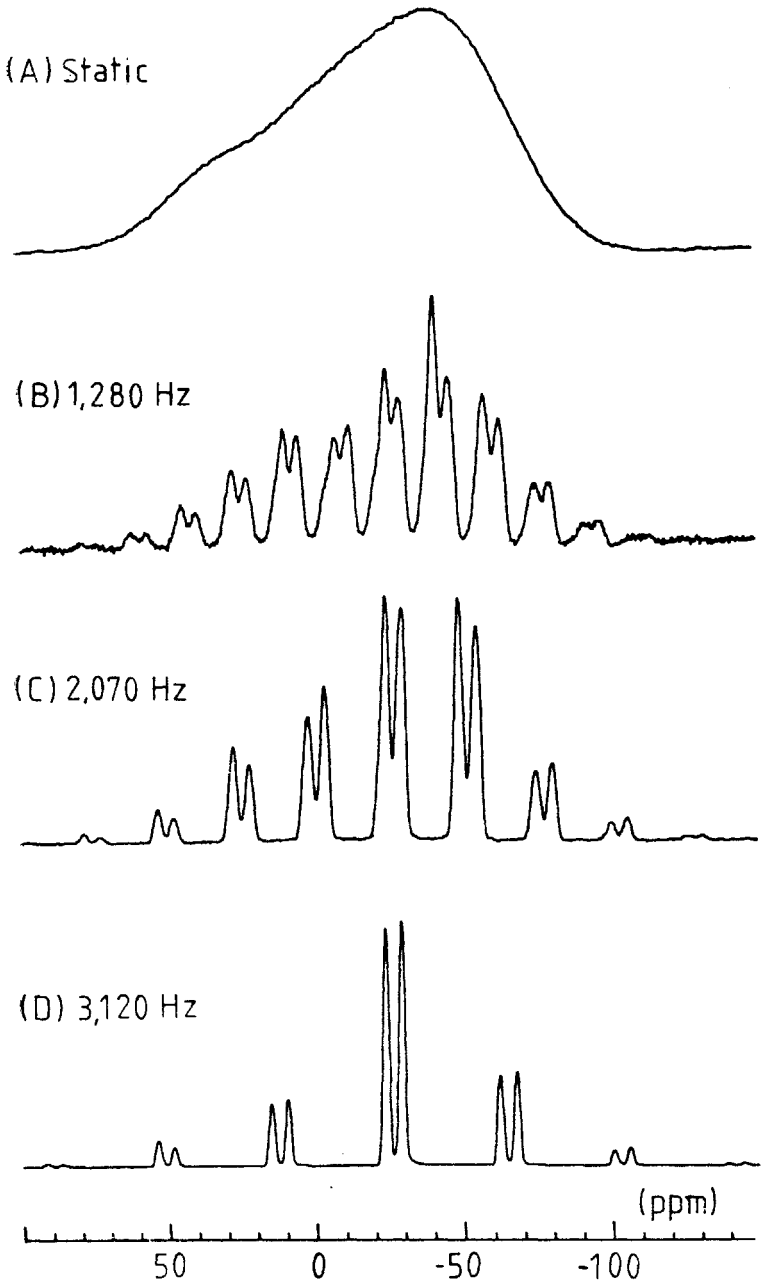

FIG 6 The ^{31}P NMR..... spectrum of $KAlP_2O_7$ as a function of spinning speed at the magic angle.[17]

moments of the nuclei, with respect to the direction of the applied magnetic field. With a powder, however, a wide range of crystallite orientations is present and a

broad envelope of resonances is observed. This is an important contribution to the broadening in most solid state spectra. Third, the presence of quadrupolar nuclei ($I > 1/2$) will also contribute to the line width. Most of the work to date has been performed on spin 1/2 nuclei, but quadrupolar nuclei with non-integral spins can also be studied by high resolution methods, because the $1/2 \rightarrow -1/2$ transition is unaffected by quadrupolar interactions, to a good approximation. Such measurements are best performed at high fields.[16]

A static ^{31}P spectrum of $KAlP_2O_7$ is shown in Fig. 6(A).[17] From such a spectrum, it is possible to extract the principal elements of the chemical shift tensor, σ_{11}, σ_{22}, σ_{33}, although this will be difficult if more than one type of phosphorus is present. The anisotropic spectrum may be averaged to the isotropic value by the technique of magic angle spinning (MAS), in which the sample is spun rapidly around and axis inclined at the so-called magic angle, $\theta = 55° 44'$, with respect to the magnetic field. The spinning speed must be comparable with the frequency spread of the shift anisotropy. The effect of increasing the spinning rate on the ^{31}P spectrum of $KAlP_2O_7$ is shown in Fig. 6. At 3120Hz, two independent phosphorus atoms, with isotropic resonances $\sigma_{iso} = 1/3\ (\sigma_{11} + \sigma_{22} + \sigma_{33})$ at -23.7 and -29.1ppm (from 80 per cent H_3PO_4) are observed. These are flanked by "spinning side bands", which are separated by the spinning speed and arise because the spinning frequency is not quite sufficient to remove all the anisotropy. It is a straightforward matter to determine the principal elements of the shielding tensor from such a spectrum, even if more than one site is present.[18]

Finally, we note that the technique of cross-polarisation (CP) can be used to increase the sensitivity of the MASNMR method to dilute nuclei.[19] The basic principle is that the magnetisation of the dilute nucleus is enhanced by coupling it to the magnetisation of an abundant nucleus, usually hydrogen. In the first application of this method by Schaefer and Stejskal,[20] the ^{13}C spectra of a series of natural polymers were greatly improved by the use of a combined CP–MAS technique. The resolution is unaffected by cross polarisation.

3.2 *Applications*

There are several ways in which MASNMR methods can contribute towards the characterisation of a polycrystalline material. If the structure is unknown, then the spectrum may reveal the number of crystallographically distinct atoms of the resonating nucleus. In the zeolite ZSM-5, for example, the ^{29}Si spectrum, reveals at least nine resonances, consistent with the space group Pnma.[21] A recent study of α-$CaZn_2(PO_4)_2$ provides another interesting illustration. The ^{31}P MASNMR spectrum (Fig. 7) shows two resonances, with isotropic shifts at 2.2 and 10.0ppm, and since the unit cell is triclinic, the structure must belong to the centrosymmetric space group $P\bar{1}$ rather than the non-centric P1.[22]

If the structure is known, the MASNMR method may provide a unique probe of any local ordering that may be present. Again, a great deal of work has been done on zeolites, where the ^{29}Si spectra are sensitive to the numbers of aluminiums

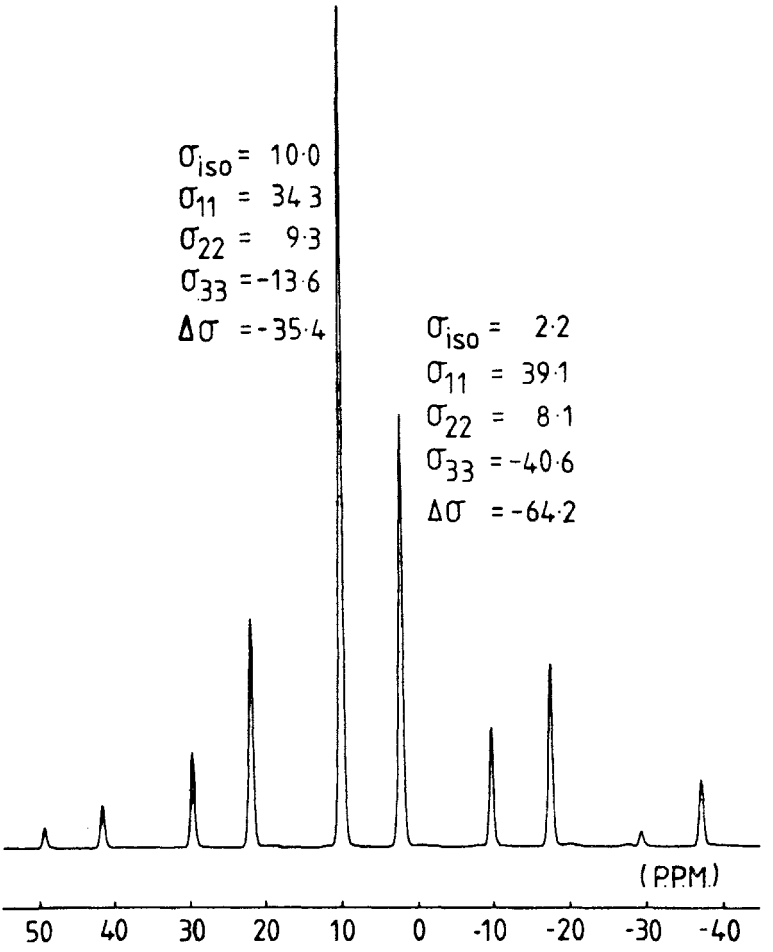

FIG 7 The ^{31}P MASNMR spectrum of α-$CaZn_2(PO_4)_2$, showing two crystallographically distinct phosphorus sites, each with spinning sidebands.[22]

in the next nearest neighbour sites.[23] This has lead, for example, to the proposal of several schemes for the ordering of silicon and aluminium in the aluminosilicate framework of zeolite-Y.[24] In a rather different example, it has been shown that the ^{31}P spectra of $Zn_{2-x}Mg_x(PO_4)_2$ solid solutions are extraordinarily sensitive to the distribution of zinc and magnesium over the two available cation sites in the structure, one of which is octahedral and the other five coordinated.[25] In other circumstances, a full refinement of the crystal structure would be needed to obtain this information.

In order to take full advantage of MASNMR data, it is necessary to be able to assign the observed peaks to particular atoms in the crystal structure, but it has proved difficult to do this because of the wide range of factors that influence the chemical shift. However, several empirical attempts have been made to relate

isotropic chemical shifts to structural features. For example, ^{29}Si shifts in minerals have been correlated with T–O–T angles,[26] Si–Si non-bonding distances[27] and with oxygen bond strengths,[28] calculated by the method of Brown and Shannon.[29] The correlation between ^{31}P chemical shifts and the bond strengths at the surrounding oxygen atoms is shown in Fig. 8.[22] Such correlations provide a useful aid to peak assignment, but further progress will depend upon a more rigorous analysis of the problem and greater use of anisotropic shift data.

But the most important area of current development, which will have a major impact on solid state chemistry, is the application of MASNMR methods to a wider range of nuclei. The list is already long, and includes ^{19}F, ^{23}Na, ^{27}Al, ^{51}V, ^{113}Cd, and ^{195}Pt, but many other nuclei have yet to be explored in detail and rapid growth can be expected in this area.

4. Powder Diffraction Methods

4.1 *Introduction*

X-ray powder diffraction methods play a central role in the study of polycrystalline materials. Data collection on a modern powder diffractometer is rapid and can yield precise *d*-spacing and intensity information. The applications of this technique are several, including :

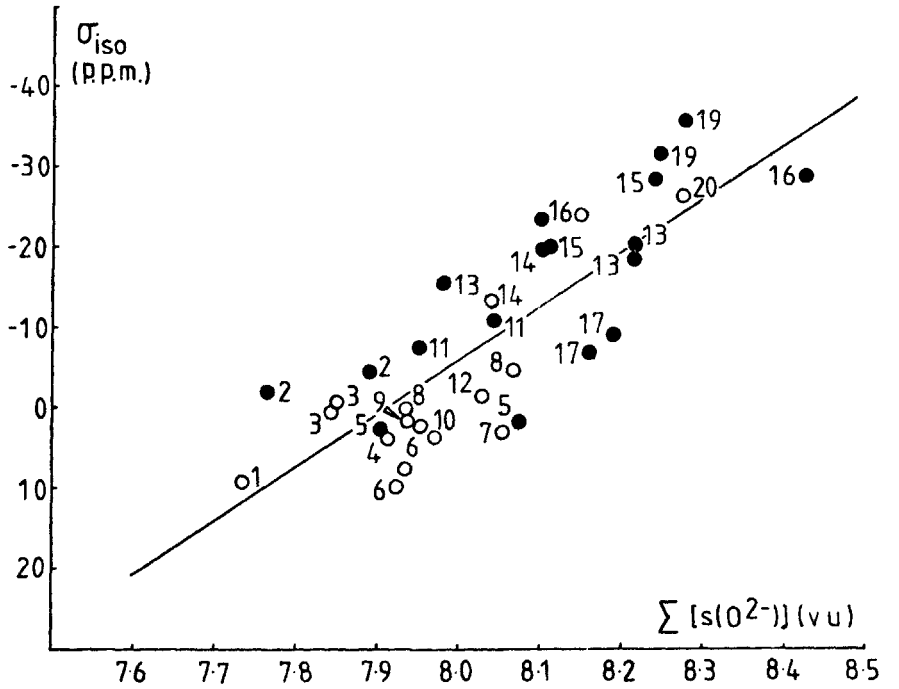

FIG 8 Plot of correlation between ^{31}P isotropic chemical shift data and bond strengths at oxygen, for a series of metal phosphates.[22]

(1) Qualitative analysis, in which the *d*-spacing data of a material are compared with values found in a comprehensive database such as the Powder Diffraction File; this can also be used in the identification of mixtures, especially with the assistance of suitable "search and match" software.

(2) Quantitative analysis of mixtures, in which the relative intensities of selected reflections of the constituent phases are compared with those in standard mixtures.

(3) Phase equilibria studies, in which the powder pattern is monitored as a function of composition or temperature.

The importance of this type of work is reflected in its widespread use, but it is essentially limited to the characterisation of known phases. New materials are, of course, routinely fingerprinted by powder X-ray diffraction, but here we examine the extent to which powder methods can yield more sophisticated information, including the crystal structure, itself. We shall consider the use of both X-rays and neutrons.

The determination of the structure, whether by single crystal or powder methods, can best be understood in terms of a series of discreet steps:

(1) indexing of the diffraction pattern and the determination of the crystal system (eg. cubic, orthorhombic, etc.) and lattice parameters;

(2) identification of the space group;

(3) solution of the phase problem and determination of the approximate structure; and

(4) refinement of the structure.

With single crystal X-ray data collected on an automatic diffractometer, this sequence of steps is normally routine. The unit cell can be identified from an automatic peak search, the space group determined from systematic absences, and the phase problem solved by Patterson or direct methods. The structure can then be refined by using a combination of least-squares and difference Fourier techniques. With powders, however, there are serious difficulties, most of which arise because of peak overlap which results when the three-dimensional intensity data is compressed into a single dimension in the powder experiment. Indexing of the reflections and unit cell determination are non-trivial, even with the aid of a good auto-indexing computer programme. These require very precise *d*-spacing data, and the use of an internal standard is recommended. Selected area electron diffraction is also of value in obtaining single crystal diffraction patterns from powder samples. Even if the cell can be found successfully, the subsequent steps may still be insurmountable. In particular, the solution of the phase problem is likely to be difficult, largely because the overlapping of adjacent reflections, which is especially marked with powder data of low symmetry systems, introduces ambiguity into the assignment of intensities to particular *hkl* values. This information is essential for both Patterson and direct methods calculations. For this reason *ab initio* structure

determination using powders has remained an empirical rather than an exact science. Some of the approaches that have been used are described in section 4.4. First, however, we shall examine the progress that has been made in the *refinement* of structures from powder data.

4.2 *Rietveld Profile Analysis*

The most striking advance in powder techniques during the last twenty years has been the advent of structure refinement by the method of Rietveld profile analysis.[30] This was initially developed for the analysis of neutron data, but, as we shall see, has also been applied to X-ray data. We have already noted that it may not be possible to determine an extensive set of integrated intensities, $I(hkl)$, from a powder profile, but Rietveld shoved that it is nevertheless feasible to refine the structure by a careful fitting of the complete profile. The lattice parameters define the 2θ value of each reflection, and an approximate model for the structure is required in order to estimate the intensities of the reflections. By assuming that the reflections are Gaussian in shape, Rietveld showed that the whole profile could be calculated and the structure then refined by a curve-fitting least-squares procedure. This important breakthrough extended the scope of powder techniques, at a stroke, from simple cubic and hexagonal systems to low symmetry materials. As an example, a refinement of the structure of Ba_2ReO_5, in space group P2/m, is shown in Fig 9.[31]

The facility with which the Rietveld method can be applied to constant wavelength neutron powder data stems largely from the simplicity of the peak shape, which is usually well described by a Gaussian function, but the method has been

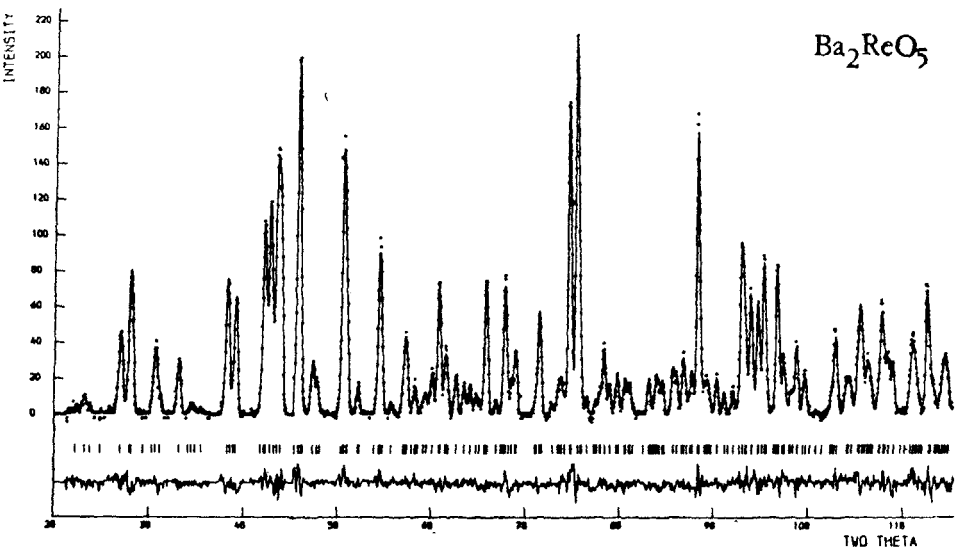

FIG 9 Observed (dots) and calculated (full line) powder neutron diffraction profiles of Ba_2ReO_5.[31] Reflection positions and a difference curve are also shown.

extended more recently to X-ray powder data[32] and time-of-flight neutron diffraction data (*see below*). It remains, however, a method by which structures are refined, and does not, in itself, provide a means of obtaining the necessary starting model. This limitation is considered in sections 4.4 and 4.5.

4.3 *Time-of-Flight Neutron Diffraction*

A conventional powder experiment employs a fixed-wavelength incident beam and a counter which measures the scattered intensity by sweeping through a range of scattering angles, 2θ. In the time-of-flight (TOF) method, the neutron beam is white and pulsed (say, 50 pulses per second). The diffraction pattern is collected by measuring the time of arrival of neutrons with different wavelengths (and, therefore, velocities) at a fixed angle counter, or time-focused counter bank (Fig. 10). This is feasible with thermal neutrons, which have velocities of approximately 10^5 cm sec^{-1}. In terms of the Bragg equation, $\lambda = 2d \sin \theta$, θ is fixed and λ is varied. A typical TOF pattern is shown in Fig. 11. As in the constant wavelength technique, Rietveld profile analysis can be performed.[33] Pulsed neutron sources for condensed matter research are available in Japan, the U.S.A., and Great Britain.

4.4 *Structure Determination with Powder Data : Empirical Methods*

The determination of structures from powder data, with or without profile analysis, has focused on obtaining starting models by one of three methods :

(1) identification of an apparently isostructural material of known structure;

(2) use of difference Fourier methods to investigate derivatives of known structures; and

(3) trial and error methods.

Method (1) is widely used, normally by means of searching the data bases for a compound with similar stoichiometry and lattice parameters to the unkown. Structures that have been determined in this way range from systems where the analogy is obvious (e.g. $Cr_2(MoO_4)_3$ and $Fe_2(MoO_4)_3$[34] to those for which a certain amount of detective work is necessary : the profile refirement of Ba_2ReO_6 which adopts the same structure as Cs_2DyCl_5, falls into the latter category (Fig 9).

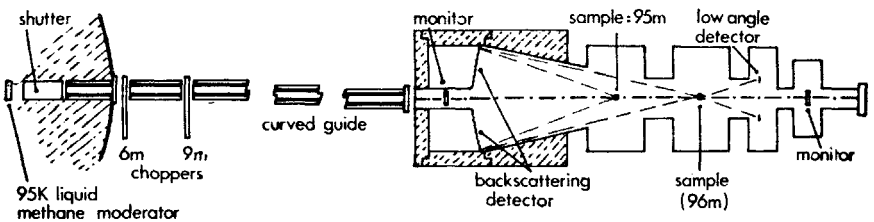

FIG 10 The high resolution powder diffractometer (HRPD) at the pulsed neutron source, ISIS, Rutherford-Appleton Laboratory, U.K. The source to sample distance is 96m. The backscattering detector bank covers the 2θ range 170-178°. Data from the different elements are time-focused in software.

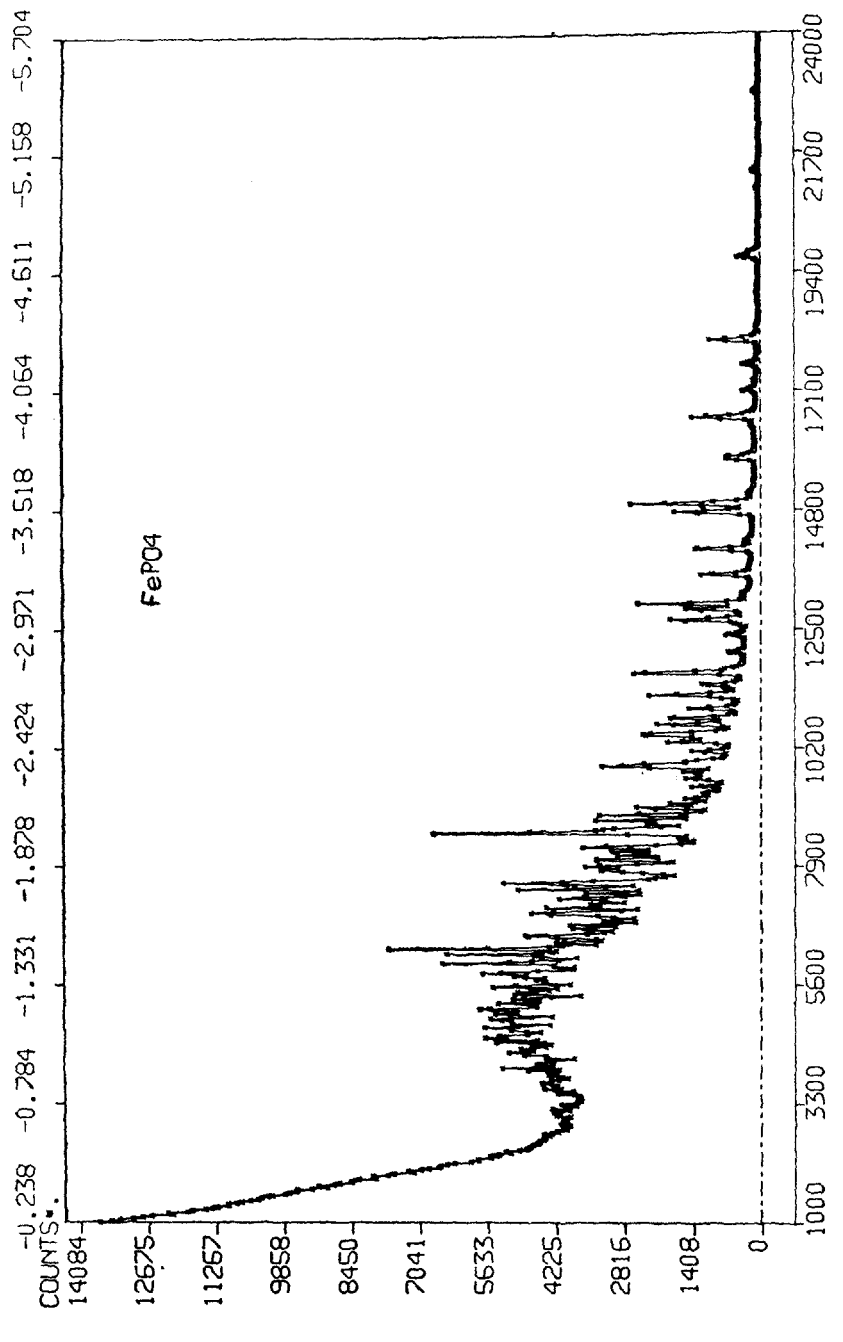

FIG 11 The TOF powder neutron diffraction pattern of $FePO_4$, collected on GPPD at the Intense Pulsed Neutron Source, Argonne National Laboratory (Battle, Harrison and Cheetham, *unpublished*). The broad feature at short times-of-flight is due to epithermal neutrons.

Method (2) has also been extensively exploited, but it suffers from the usual problem with powders: there is a dearth of discreet integrated intensity information. However, when most of the atom positions have been located and refined, the Rietveld procedure provides a list of approximate observed $I(hkl)$'s which can be used with the calculated $I(hkl)$'s in a difference Fourier calculation. This approach should be used with caution, but it has been applied successfully to some interesting problems such as the location of adsorbed molecules in zeolite cages[35] and the positions of protons in complex oxides.[36] This strategy is enormously valuable in solid state chemistry, but, like method (1), it is obviously unsuitable for the characterisation of entirely new structure types.

For entirely new structures, workers have been forced to rely on trial and error approaches. This has usually involved the use of both X-ray and neutron data, the former being used to determine heavy atom positions from radial distribution functions. The work of Taylor on uranium tetrabromide provides a good example; uranium was located with X-rays and the lighter halogen atoms were positioned by trial and error using neutron data.[37] In another instance, the same methodology was used to solve the non-centrosymmetric superstructure of Bi_3ReO_8.[38] This approach to structure solving, whilst sometimes unavoidable, is extremely time consuming and frequently unrewarding. In the following section, we shall describe some of the very latest developments that promise to take powder methods into a new and exciting phase in which trial-and-error procedures will become redundant.

4.5 *Ab Initio Stucture Determination with Powder Data*

We have already noted that the main loss of information in a powder experiment arises from the overlapping of adjacent Bragg reflections which leads to ambiguities in their intensities. This information is essential if the classical methods of structure solving, used routinely in single crsytal work, are to be employeg. The new generation of powder diffractometers, at both neutron facilities and synchrotron sources, have such high resolution that this limitation should be largely overcome. The improvement in resolution leads to a dramatic reduction in the incidence of peak overlap. Indeed, the instrumental resolution is now so good (ed. $\Delta d/d = 0.04$ per cent on the high resolution powder diffractometer (HRPD) at the Rutherford Laboratory, U.K.), that most samples show line broadening due to particle size and strain effects.

This promise has yet to be fulfilled, but the feasibility of solving known structures from powder data by using direct methods has been demonstrated,[39] and one of the first experiments on HRPD illustrates what might be done with unknown structures. The material studied was $FeAsO_4$, which was first reported by Shafer *et al.*[40] Subsequently, D'Yvoire indexed the X-ray powder pattern according to a monoclinic cell, assigned the space group P 2(1)/*n*, and on the basis of infrared evidence and the facile transformation of the monoclinic modification to one with the $CuSO_4$ structure, suggested that the iron atom might be octahedrally coordinated.[41] Data for $FeAsO_4$, collected on HRPD at the Spallation Neutron Source

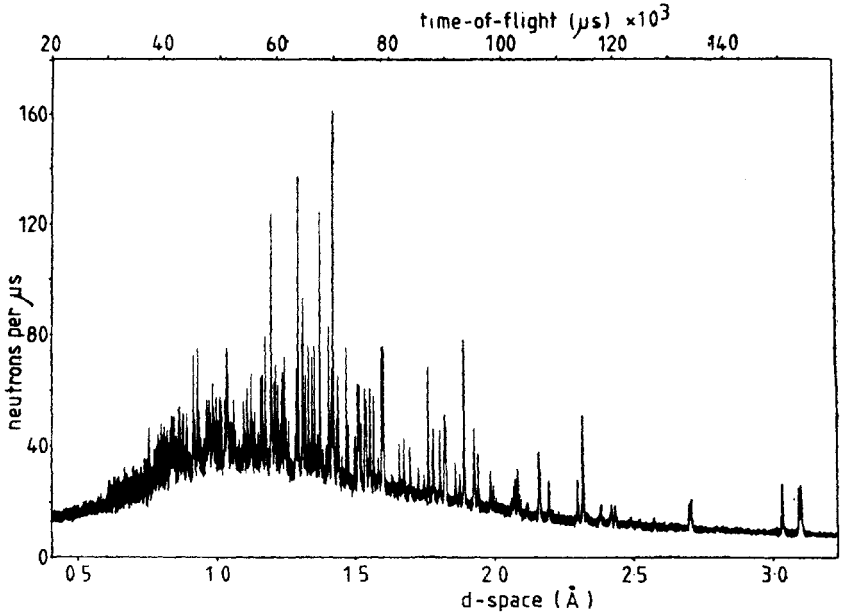

FIG 12 The TOF powder neutron diffraction pattern of $FeAsO_4$, collected on HRPD at ISIS.[5] Note the extraordinary resolution. The epithermal neutrons, which are seen in the pattern of $FePO_4$ (Fig. 11) are removed by the neutron guide.

(ISIS) are shown in Fig. 12.[5] The correctness of the cell proposed by D'Yvoire was first confirmed by auto-indexing of the pattern using the programme FZON,[42] and the lattice parameters were then refined and the space group confirmed by examining the systematic absences. Integrated intensities, $I(hkl)$, were then obtained manually for 139 reflections, including approximately 60 weak reflections. It is this stage that is facilitated by high resolution, since peak overlap, which normally leads to ambiguities in the intensities of individual Bragg reflections, is minimised. Structure factor amplitudes were then calculated according to the relationship:

$$I(hkl) = \lambda^4 m F(hkl)^2,$$

where m is the multiplicity of reflection hkl and λ is the wavelength at which it is measured. The $F(hkl)$ values were then used as the input for direct methods analysis using the programe MITHRIL.[43] Neutron data are normally well suited to direct methods analysis because neutron scattering length fall within a narrow range of values. In the $FeAsO_4$ analysis, both triplets and negative quarters were calculated. The peak list from the calculation with the highest figure of merit is shown in Table I. Analysis of the interpeak distances and angles confirmed that a chemically sensible solution had been found, with peaks 1 and 2 corresponding to Fe and As, respectively, and peaks 3–6 to oxygen. Note that the peaks appear in order of their neutron scattering lengths and that there is a substantial gap between peaks 6 and 7; the latter indicates the level of noise in the map. The coordi-

nates obtained from the direct methods analysis were then refined to yield the structure shown in Fig. 13. One of the interesting features of the structure of $FeAsO_4$ which, surprisingly, is isostructural with $LiAlH_4$, is the presence of five coordinated iron sites which share a common edge.

TABLE I

Direct methods solution for $FeAsO_4$

Peak No.	x	y	z	height
1	0.322	0.051	0.242	2691
2	0.925	0.179	0.257	1960
3	0.369	0.244	0.087	1320
4	0.485	0.127	0.631	1199
5	0.102	0.046	0.322	1193
6	0.790	0.080	0.087	1104
7	0.062	0.087	0.726	591
8	0.885	0.117	0.887	590

No. of reflections = 139.
Triplets generated from top 66 reflections.
Negative quartets generated from top 67 reflections.

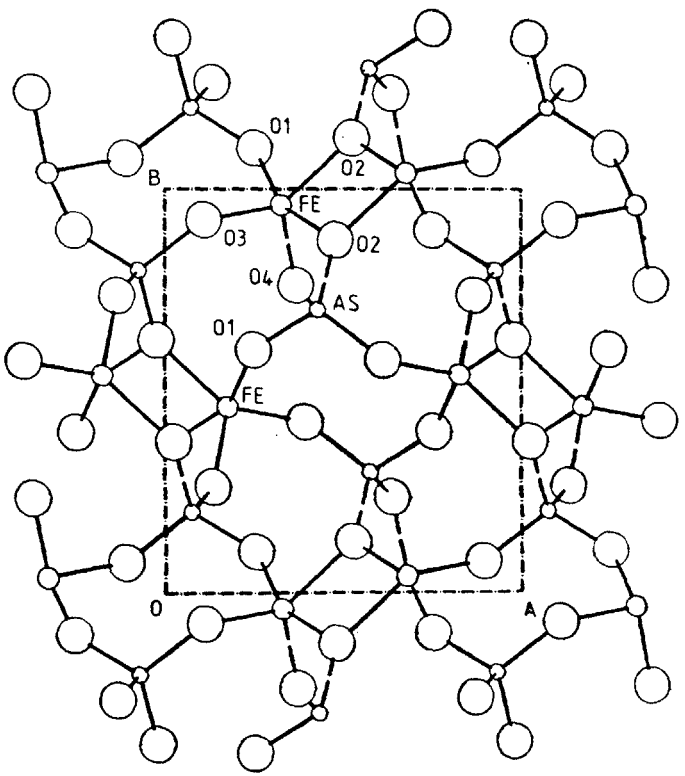

Fig 13 The crystal structure of $FeAsO_4$, viewed down [001].

Recent developments in high resolution X-ray instrumentation suggest that similar progress can be expected in this area, and at the time of writing, the crystal structure of α-$CrPO_4$ has just been determined from synchrotron powder data obtained at the National Light Source, Brookhaven.[44] The orthorhombic structure, with 8 atoms in the asymmetric unit, was solved by Patterson methods by using a vector search procedure.

The success of these very recent works augurs well for future structure determination with powders. Direct methods will no doubt, be preferred with neutron data, but the use of Patterson techniques should not be neglected as a means of locating strong scatterers. High resolution X-ray data should be amenable to both approaches. Single crystal methods will continue to be the preferred medium for structure determination; but powder techniques now offer a viable alternative.

4.6 *Applications*

The applications of powder methods to structure determination, mainly using the empirical methods described in section 4.4, are varied and increasingly numerous, and the use of the Rietveld method has grown from a handful of paper per annum in the early 70's to 150 in 1984. Applications to solid state chemistry were reviewed by Cheetham and Taylor in 1977[45] and more recently by Hewat,[46] who referenced approximately 250 studies on oxides, hydrides, halides, alloys, and minerals. The bulk of the work has involved neutron diffraction, for which the treatment of the peak shape is more straightforward, but X-ray Rietveld analysis is increasingly popular, especially with the availability of more sophisticated computer programmes. For example, Baerlocher[47] has developed a programme that incorporates slack constraints, of the type described by Hendrickson and Konnert,[48] into the least-squares refinement. This has been used to refine complex zeolite structures such as that of ZSM-5.[49]

One measure of the scope of structure determination with powder data is the complexity of the problems that can now be tackled. The current state of the art is that structural models with about 100 parameters can be refined,[34,50] but the new generation of ultra-high resolution diffractometers is expected to increase this limit to 3–400. A recent study of potassium zeolite-L, containing pyridine, illustrates the sophistication of the problems that are now within reach.[51] The position and orientation of the organic molecule inside the zeolite channel was determined at 4K (Fig. 14) and the results confirmed by means of molecular mechanics calculations; the experimental and calculated positions of the molecule agreed within 0.2Å.

The future prospects for powder diffraction are extremely exciting. The use of high resolution methods for the *determination* of structure has already been described (section 4.5), but equally, promising is the utilization of high intensity sources for time-resolved experiments. With existing facilities, medium resolution neutron or X-ray diffraction patterns can be collected in a matter of minutes, but new sources will enable experiments to be performed in seconds, making possible the study of solid state reactions and other processes in real time.

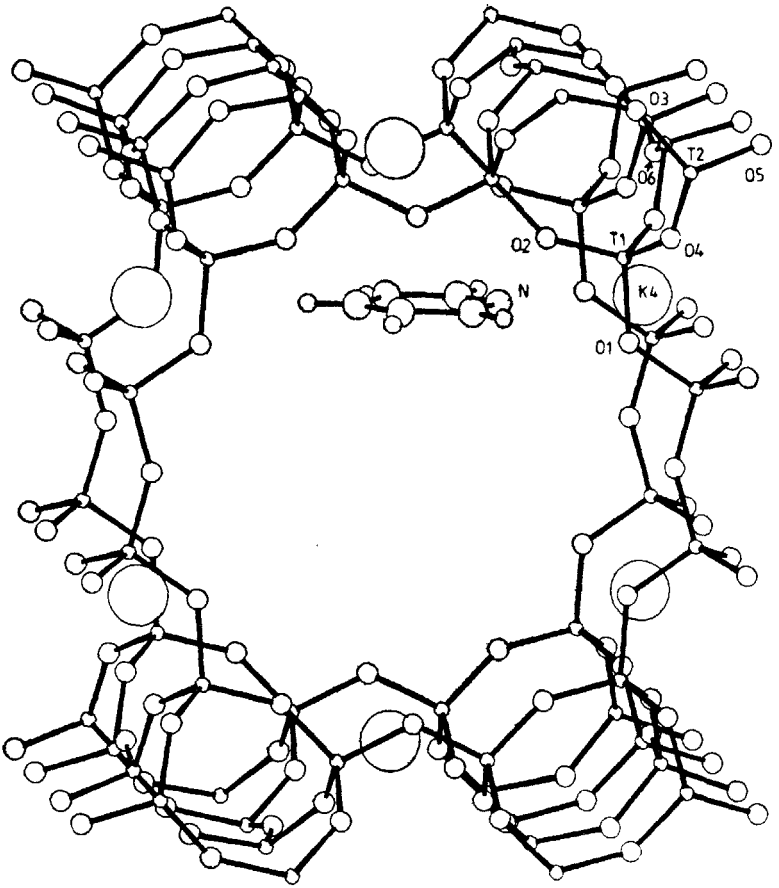

FIG 14 The location of pyridine in the main channel of potassium zeolite-L.[51] Note that the molecule lies close to the wall of the channel, optimising short range interactions, whilst enjoying an acid-base interaction with the potassium, K(4).

5. CONCLUSIONS

This brief review of some of the methods that are now being used to study powders has inevitably been selective. Many important techniques, such as Mössbauer spectroscopy and EXAFS, have been omitted, but attention has focused on those methods that have widespread applicability and where the recent developments have been most striking. One important omission is high resolution electron microscopy (HRTEM). The availability of high energy (3–400 KeV) transmission instruments with improved objective lenses has brought the resolving power of the electron microscope down to the atomic level, thus offering an alternative means of structural characterisation for powders. It should be noted that an HRTEM image represents a projection of the structure down the axis of viewing, and is therefore ideal for studying new structure with a short crystallographic axis. This has been demonstrated as a means of characterising new phases,[52] especially when it is com-

bined with image simulations,[53] but it is best applied to the study of materials of known architectural type, such as the niobium oxide block phases. For entirely new structure types, modelling by trial-and-error methods is necessary. In addition, it should be noted that HRTEM does not yield atomic coordinates, and therefore bond lengths and bond angles, with the precision that is obtainable with X-ray and neutron diffraction. Nevertheless, in some areas, it is pre-eminent, especially in the study of structural defects.

We have noted not only the strengths of the techniques that have been described, but also their limitations, thus underlining the weakness of a single pronged attack on the characterisation of materials. The complementarity of the methods that are now available, however, is self-evident, and the most efficacious approach to a problem is likely to be one that harnesses the advantages of several techniques. When subjected to a multifaceted attack of this type even the most stubborn of problems is likely to yield.

REFERENCES

1. *Synthesis and Characterisation of Advanced Materials* National Research Council (National Academy Press Washington D C 1984)
2. J B Goodenough H Y-P Hong and J A Kafalas *Mater Res Bull* **11** (1976) 203
3. A Clearfield R Guerra A Oskarsson M A Subramanian and W Wang *Mater Res Bull* **18** (1983) 1561 and references therein
4. A K Cheetham and A J Skarnulis *Anal Chem* **53** (1981) 1060
5. A K Cheetham W I F David M M Eddy R J B Jakeman M W Johnson and C C Torardi *Nature* **320** (1986) 46
6. E R Andrew *Progr NMR Spectrosc* **8** (1971) 1
7. T G Sparrow B G Williams C N R Rao and J M Thomas *Chem Phys Lett* **108** (1984) 547
8. A R Rae-Smith and A K Cheetham *J Solid State Chem* **30** (1979) 345
9. A K Cheetham A J Cole and G J Long *Inorg Chem* **20** (1981) 2747
10. A K Cheetham and A R Rae-Smith *Mater Res Bull* **16** (1981) 7
11. G Cliff D M Maher and D C Joy *J Microsc* **136** (1984) 219
12. A K Cheetham A J Skarnulis D M Thomas and K Ibe *J chem Soc chem Commun* (1984) 1603
13. R F Egerton *Phil Trans R Soc* **305** (1982) 521
14. C N R Rao T G Sparrow B G Williams and J M Thomas *J chem Soc chem Commun* (1984) 1238
15. E R Andrew A Bradbury and R G Eades *Nature* **182** (1958) 1659
16. S Ganapathy S Schramm and E Oldfield *J chem Phys* **77** (1982) 4360
17. R J B Jakeman *personal communication*
18. M M Maricq and J S Waugh *J chem Phys* **70** (1972) 3300
19. A Pines M C Gibby and J S Waugh *J chem Phys* **56** (1979) 1776
20. J Schaefer and E O Stejskal *J Am chem Soc* **98** (1976) 1031
21. J M Thomas J Klinowski S Ramdas B K Hunter and D T B Tennakoon *Chem Phys Lett* **102** (1983) 158
22. A K Cheetham N J Clayden C M Dobson and R J B Jakeman *J chem Soc chem Commun* (1986) 195
23. E Lippmaa M Magi A Samoson G Engelhardt and A R Grimmer *J Am chem Soc* **102** (1980) 4889

24. M T Melchior D E W Vaughan and A J Jacobson *J Am chem Soc* **104** (1982) 4859
25. R J B Jakeman A K Cheetham N J Clayden and C M Dobson *J Am chem Soc* **107** (1985) 624a
26. J V Smith and C S Blackwell *Nature* **303** (1983) 223
27. S Ramdas and J Klinowski *Nature* **308** (1984) 521
28. K A Smith R J Kirkpatric E Oldfield and D M Henderson *Am Min* **68** (1983) 1206
29. I D Brown and R D Shannon *Acta Cryst* A**29** (1973) 226
30. H M Rietveld *J appl Cryst* **2** (1969) 65
31. D M Thomas and A K Cheetham *unpublished results*
32. G Malmros and J O Thomas *J appl Cryst* **10** (1977) 7
33. R B Von Dreele J D Jorgensen and C G Windsor *J appl Cryst* **15** (1982) 581
34. P D Battle A K Cheetham W T A Harrison N J Pollard and J Faber *J Solid State Chem* **58** (1985) 221
35. A N Fitch H Jobic and A Renouprez *J chem Soc chem Commun* (1985) 284
36. F J Rotella J D Jorgensen R M Biefeld and B Morosin *Acta Cryst* B**38** (1982) 1697
37. J C Taylor and P W Wilson *Acta Cryst* B**30** (1974) 2664
38. A K Cheetham and A R Rae-Smith *Acta Cryst* **B41** (1985) 225
39. A N Christensen M S Lehmann and M Nielsen *Aust J Phys* **38** (1985) 497
40. E C Shafer M W Shafer and R Roy *Z Krist* **108** (1956) 263
41. F D'Yvoire *C r* **275**C (1972) 949
42. J W Visser *J appl Cryst* **2** (1969) 89
43. C J Gilmore *J appl Cryst* **17** (1984) 42
44. J P Attfield A W Sleight and A K Cheetham *to be published*
45. A K Cheetham and J C Taylor *J Solid State Chem* **21** (1977) 253
46. A W Hewat *Chem Scripta (in Press)*
47. Ch Baerlocher *The X-ray Rietveld System* XRS82; ETH Zurich (1982)
48. J H Konnert and W A Hendrickson *Acta Cryst* A**36** (1980) 344
49. Ch Baerlocher *Proc 6th int Zeolite Conf* Reno, U.S.A (1984) 833
50. B J Hathaway and A W Hewat *J Solid State Chem* **51** (1984) 364
51. P A Wright J M Thomas A K Cheetham and A K Nowak *Nature* **318** (1985) 611
52. D A Jefferson J M Thomas M K Uppal and R K Grasselli *J chem Soc chem Commun* (1983) 594
53. A J Skarnulis *J appl Cryst* **12** (1979) 636